

Inelastic incoherent neutron scattering study of the methyl rotation in various methyl halides

M. Prager, J. Stanislawski, Wolfgang Häusler

Angaben zur Veröffentlichung / Publication details:

Prager, M., J. Stanislawski, and Wolfgang Häusler. 1987. "Inelastic incoherent neutron scattering study of the methyl rotation in various methyl halides." The Journal of Chemical Physics 86 (5): 2563–75. <https://doi.org/10.1063/1.452059>.

Nutzungsbedingungen / Terms of use:

licgercopyright

Dieses Dokument wird unter folgenden Bedingungen zur Verfügung gestellt: / This document is made available under the following conditions:

Deutsches Urheberrecht

Weitere Informationen finden Sie unter: / For more information see:

<https://www.uni-augsburg.de/de/organisation/bibliothek/publizieren-zitieren-archivieren/publizieren>



Inelastic incoherent neutron scattering study of the methyl rotation in various methyl halides

Cite as: J. Chem. Phys. **86**, 2563 (1987); <https://doi.org/10.1063/1.452059>

Submitted: 21 August 1986 • Accepted: 24 November 1986 • Published Online: 04 June 1998

M. Prager, J. Stanislawski and W. Häusler



[View Online](#)



[Export Citation](#)

ARTICLES YOU MAY BE INTERESTED IN

[Methyl quantum rotation in solid CH₃F: An inelastic neutron scattering study](#)

The Journal of Chemical Physics **89**, 1181 (1988); <https://doi.org/10.1063/1.455227>

[Learn More](#)

The Journal of Chemical Physics **Special Topics** Open for Submissions

Inelastic incoherent neutron scattering study of the methyl rotation in various methyl halides

M. Prager and J. Stanislawski

Institut für Festkörperforschung der KFA, D-5170 Jülich, West Germany

W. Häusler

Institut für Theoretische Physik der Universität, Glückstrasse 6, D-8520 Erlangen, West Germany

(Received 21 August 1986; accepted 24 November 1986)

The inelastic incoherent neutron scattering technique has been applied in an energy range from $0.4 \mu\text{eV}$ to 60 meV to measure the rotational excitations of the methyl groups in polycrystals of CH_3I , CH_2DI , CD_3I , CH_3Br , CD_3Br , and CH_3Cl in a temperature range $5 < T[\text{K}] < 190$. Tunnel splittings of the librational ground state of 2.44 and $0.9 \mu\text{eV}$ were found for CH_3I and CH_3Br , respectively. Excitations to the higher excited librational states are identified via the temperature dependence and the isotope effects of the modes in the meV regime. The rotor-rotor coupling between neighboring methyl groups is found to be small. Thus single particle rotational potentials were derived from the observed eigenenergies. The potential strength increases going from the iodide via the bromide to the chloride. In CH_3Br the rotational potential does not change on deuteration. In CH_3I a very unusual increase in the rotational potential with deuteration is found. Besides the methyl librations, large amplitude motions around axes perpendicular to the molecular symmetry axis are observed at energies comparable to the methyl libration. The coupling of the methyl rotor to lattice modes modulating the strength of the orientational potential in CH_3I gives rise to a peculiar temperature dependence of the tunnel splitting.

I. INTRODUCTION

The methyl halides are the simplest molecules containing CH_3 groups and thus among the most simple molecules. They represent a symmetric prolate top, with a small moment of inertia being equal to that of the CH_3 group. Methyl iodide has only one solid phase, methyl bromide shows two solid phases.^{1,2} Besides the low temperature phase, there is a second solid phase stable from 5.7 deg below the melting point. The low temperature structures of both compounds are isomorphous: $Pnma$ with $Z = 4$ and the molecules at c sites. If the CH_3 group is replaced by the corresponding halogen, this structure is almost identical to that of solid I_2 or Br_2 .³ A projection of the structure on the a - c plane is shown in Fig. 1. The molecules are arranged in the c direction as inclined chains in an antiferromagnetic order if we characterize the molecular orientation by a spin variable. The second solid phase of methyl bromide is isomorphous to methyl chloride.⁴ Here the center of mass structure is the same as in the iodide but the molecular orientations now represent a ferromagnetic arrangement. As a consequence of this one finds the space group $Cmc2_1$ with $Z = 2$.

Various reasons make the methyl iodide and bromide interesting from the point of view of methyl group rotation. (i) Because of the molecular symmetry there is no intramolecular hindering potential. The methyl rotation is identical with the overall rotation of the whole molecule around its small axis of inertia. The rotational potential thus fully originates from the interaction with neighboring molecules. (ii) The crystal structure suggests that the rotational excitations might represent an example of linear chains of interacting methyl groups which is an extension of the case of pairs of coupled CH_3 groups observed in lithium acetate⁵ and di-

methyl tin dichloride.⁶ (iii) Due to the much simpler structure of the methyl halides there is a hope to understand the system on the base of intramolecular forces. (iv) The temperature behavior of the tunneling modes, i.e., their coupling to phonons,^{7,8} might be especially simple because the libration of the methyl group is an external mode. In force models available for molecular crystals^{9,10} it can be determined from a symmetry analysis which phonons interact with the methyl rotation. Thus not the full density of states⁷ but individual phonon branches may be of importance. This could stimu-

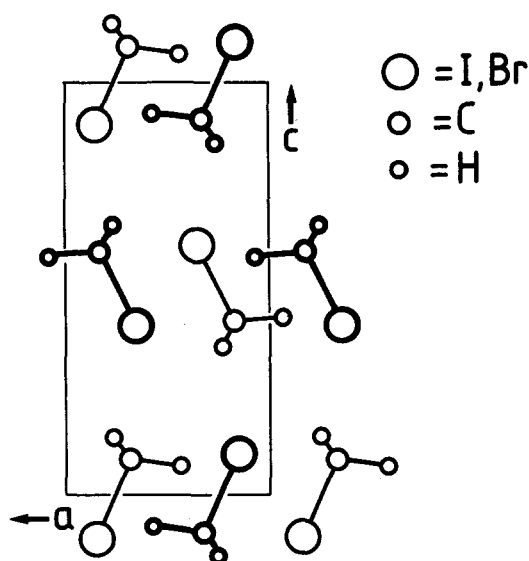


FIG. 1. Projection of the structure of CH_3I on the a - c plane according to Ref. 1. Large circles: I, medium size circles: C, small circles: H, D.

late new theoretical efforts. (v) The lattice dynamics of molecular crystals consisting of polar molecules is actually a very active field.^{10,11} Models which describe the intermolecular interaction as a superposition of, for example a Lennard-Jones and dipole-dipole interactions should describe the rotational potential for the methyl group *ab initio* and thus give an additional experimental quantity beside the dispersion curves to test such calculations. Thus the methyl halides might be a candidate for a model system in this new field. Due to the simplicity of the molecules and the crystal structure, the methyl halides have attracted a great deal of interest for decades.¹²⁻²² In the very first studies of the infrared spectra^{12,13} the data were already interpreted on the basis of dipole-dipole and atom-atom interactions. However, the crystal structures of the bromide and iodide were not known at this time. In the meantime further investigations of the IR, FIR, and Raman spectra have been undertaken down to temperatures $T = 20$ K.^{15,20,21} The spectra are interpreted in a group theoretical analysis based on the known molecular and crystal structures.¹ The small shift of the internal modes is interpreted on the basis of van der Waals type intermolecular interactions with no influence of hydrogen bonds.

While IR and Raman spectra only display the excitations at $Q = 0$, inelastic incoherent neutron scattering data sample the excitations in the whole Brillouin zone. The only neutron scattering experiment (on CH_3I) known to us¹⁹ was concentrating on the effects of multiphoton processes in neutron spectra of molecular substances and not in determining the rotational potentials.

It is the scope of this paper to present, as a first step toward an increased understanding of methyl halides, the

incoherent inelastic neutron scattering spectra measured in a very wide range of energy transfers $0.4 \mu\text{eV} < E < 60 \text{ meV}$. The spectra are mainly evaluated with respect to the methyl rotational potentials. Special attention is given to isotope effects which also are evaluated for the assignment of the transition energies. For this purpose the effect of temperature was also used, since librations usually broaden faster with increasing temperature than acoustic phonons because of the anharmonicity of the rotational potential.²³

II. EXPERIMENTS AND RESULTS

The sample materials were obtained from various companies (Ega, Aldrich, Merck, MSD Isotopes). The protonated materials had a purity of 99.9%, the deuterated ones of 99%. All materials were used in the experiments without further purification.

The high resolution experiments were performed at the backscattering spectrometer IN10 at the ILL, Grenoble,²⁴ using the best obtainable energy resolution $\delta E_{\text{el}} = 0.4 \mu\text{eV}$. The energy range $2 < E [\text{meV}] < 60$ was investigated with the thermal time of flight spectrometer SV22,²⁵ using various combinations of incoming neutron energy and energy resolution. These last spectra are all measured in energy loss of the neutrons.

A. Methyl iodide

1. CH_3I

The spectrum of CH_3I measured with an energy resolution of $\delta E_{\text{el}} = 2.0 \text{ meV}$ is dominated by one strong inelastic line at about 13.9 meV (Fig. 2). This line has a finite width of about 1 meV. Besides this prominent line there is some unresolved intensity near the elastic line and a double peak at energies of about twice that of the dominant line. Using an increased energy resolution (Fig. 3) the dominant line is

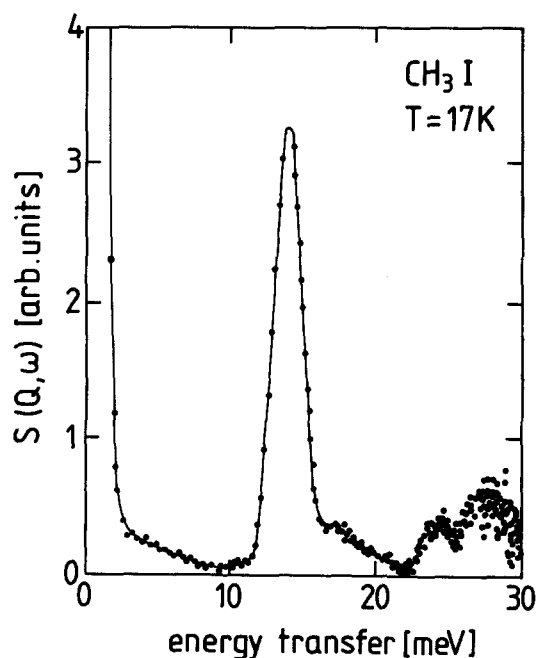


FIG. 2. Scattering function $S(Q, \omega)$ of CH_3I as derived from neutron time of flight spectra after standard corrections using a spectrometer setup with a neutron wavelength $\lambda_0 = 1.51 \text{ \AA}$ and an elastic energy resolution $\delta E_{\text{el}} = 2.0 \text{ meV}$. All detectors between $\theta_{\text{min}} = 10^\circ$ and $\theta_{\text{max}} = 130^\circ$ are summed up. Instrument: SV22 at the FRJ2 in Jülich.

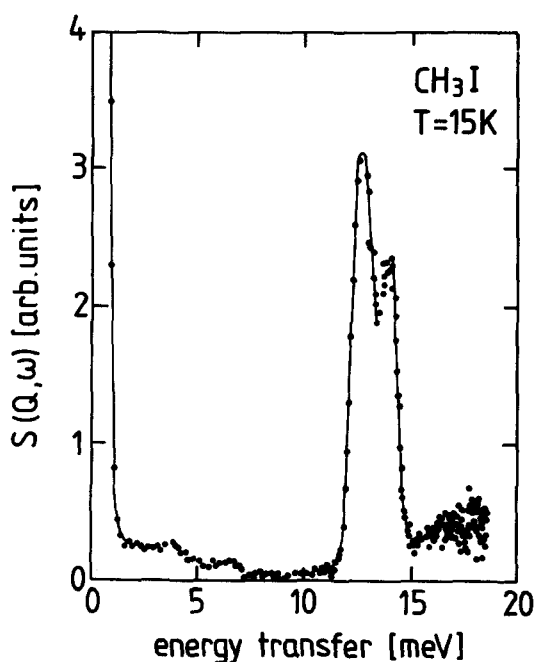


FIG. 3. As Fig. 2 but $\lambda_0 = 1.82 \text{ \AA}$ and $\delta E_{\text{el}} = 0.8 \text{ meV}$.

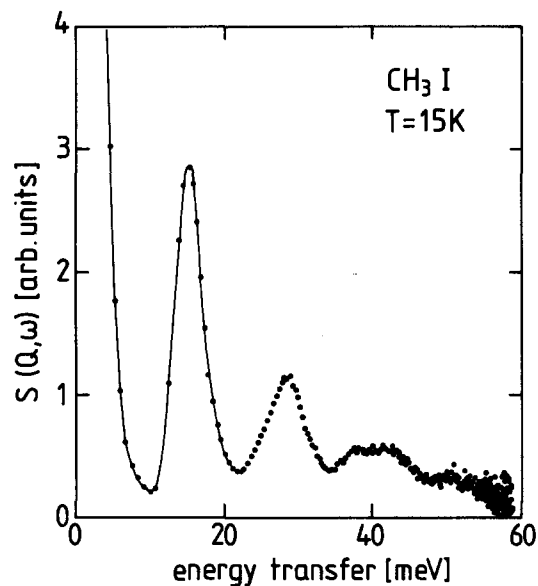


FIG. 4. As Fig. 2 but $\lambda_0 = 1.08 \text{ \AA}$ and $\delta E_{el} = 5.0 \text{ meV}$.

found to be at least a doublet, with the peak at lower energy transfer 13.27 meV having an intrinsic width. In the low energy region some peaks in the density of states are now well resolved. Increasing the range of energy transfers available at the cost of good energy resolution we observe some further transitions (Fig. 4) which obviously are multiplets. The peak at about 28 meV was partly observed in Fig. 2 and consisted there of two lines. It is now found to have a shoulder at higher energy transfers. The broad structure around 40 meV also contains various lines. Since the energy resolution increases at large energy losses of the neutrons and since the excitation energies are much better defined at low temperatures, these spectra contain much better defined structures than those measured earlier with neutron energy gain.¹⁹ The results are in good agreement, however. The peak positions of the various excitations are listed in Table I. For comparison the energies obtained in the most recent Raman and IR study²¹ are also shown. With increasing temperature all modes shift to smaller energies. The effect is more pronounced for the very low lying shallow peaks than for the two prominent ones. Some values for $T = 57 \text{ K}$ are shown in column 2 of Table I. The two prominent peaks, furthermore, strongly decrease in intensity with increasing temperature in such a way that the low energy transition at 13.27 meV becomes less pronounced relative to the 14.54 meV peak at high temperatures. All results are summarized in Fig. 5 which represents the transition energies and intensities as they change with the sample temperature.

The high resolution spectrum of CH_3I shows a tunneling peak of resolution width at an energy transfer $\hbar\omega_t = 2.44 \text{ meV}$ (Fig. 6). Spectra were recorded at two values of momentum transfer $Q = 1.40$ and 1.88 \AA^{-1} . At $Q = 1.40 \text{ \AA}^{-1}$ the intensity ratio between the inelastic line and the elastic one is determined to be $I_{inel}/I_{el} = 0.24$. The width Γ_t [FWHM] of the tunneling peak is resolution determined. Taking into account the statistical error of the data we can estimate an upper limit $\Gamma_t/\hbar\omega_t < 0.02$.

TABLE I. Peak positions in the density of states of CH_3I as measured by inelastic neutron scattering technique at two temperatures. Raman and infrared data of Ref. 21 are given for comparison. For further literature values see the reference. All energies are given in meV. The assignment of the rotary modes of the molecule are given by the symbols (see the text).

$T = 15 \text{ K}$	This work		Ref. 21	
	INS	57 K	Raman 20 K	Infrared 20 K
4.0		3.8	3.4 4.2	
			6.1 6.3	4.65
7.0		6.8	7.7 13.26 R_x, R_y	7.13
13.27 R_z		13.05	13.44 R_x, R_y	13.88
			14.19 R_z 14.44 R_x, R_y	
14.54 R_x, R_y		14.24	14.56 R_x, R_y	14.93 15.49
			17.47 18.84 20.32	
24.2 R_z			23.17	23.3
27.6			24.28	24.4
37.5–44.0			27.76	
50.3				

The temperature dependence of the tunneling lines was measured in the range $3.8 < T[\text{K}] < 35.8$. The spectra were fitted by a scattering function consisting of one δ function and three Lorentzians of equal intensity at energy transfers $\hbar\omega_t$, $-\hbar\omega_t$, and zero,²⁶ all lines being convoluted with the resolution function. The tunneling splitting behaves quite unusually (Table II, Fig. 7): after a small increase up to 2.59

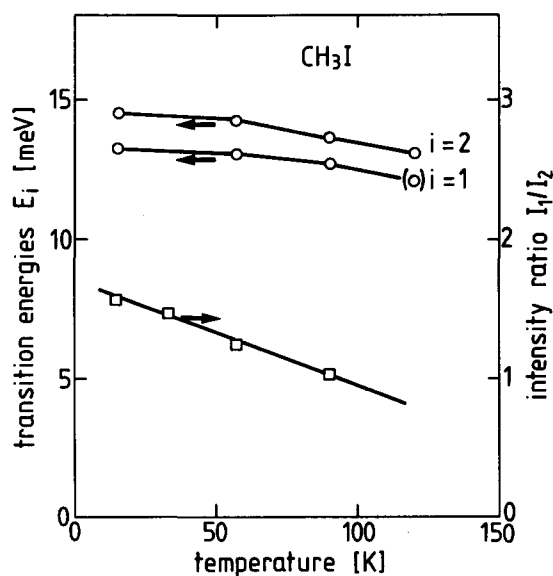


FIG. 5. Temperature dependence of the transition energies E_i and the relative intensity of the two sublines in the intense doublet of CH_3I .

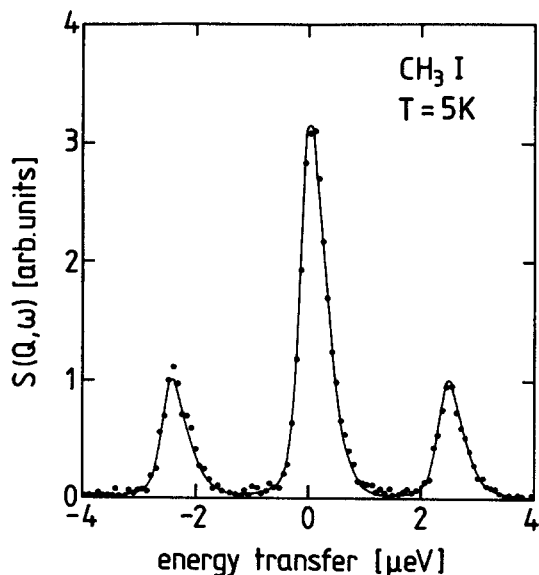


FIG. 6. Scattering function $S(Q, \omega)$ of CH_3I in the μeV energy range. The tunneling transitions are represented by the two inelastic lines at $\hbar\omega_{\text{tun}} = \pm 2.44 \mu\text{eV}$. The momentum transfer is $Q = 1.88 \text{ \AA}^{-1}$, the instrumental resolution $\delta E_{\text{el}} = 0.40 \mu\text{eV}$.

TABLE II. Tunnel splittings $\hbar\omega_t$ and linewidths Γ_t of the methyl group in CH_3I at various temperatures T .

$T[\text{K}]$	$\hbar\omega_t [\mu\text{eV}]$	$\Gamma_t [\mu\text{eV}]$
3.72	2.44	...
5.34	2.45	...
16.0	2.59	(0.05)
22.5	2.58	0.10
28.5	2.27	0.48
30.7	2.07	0.78
35.8	1.31	1.51

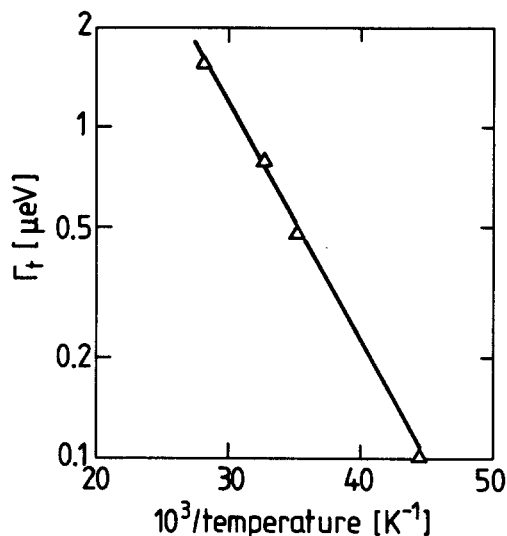


FIG. 8. Width of the tunneling lines in CH_3I as a function of temperature represented in an Arrhenius plot.

μeV at $T = 20 \text{ K}$ it decreases in the usual way. If we distinguish two different activation energies for the increase and the decrease of $\hbar\omega_t$, respectively (compare discussion in Sec. III A 3) we find $E_a^{\text{increase}} = 2.1 \text{ meV}$ and $E_a^{\text{decrease}} = 13.0 \text{ meV}$ (solid line of Fig. 7). The broadening of the tunneling lines obeys very well an Arrhenius law (Fig. 8) with an activation energy $E_a = 14 \text{ meV}$.

2. CD_3I

Because of the strong isotope effect in rotational tunneling,²⁶ tunneling transitions for CD_3I will be far out of the range of any neutron spectrometer. Thus we measured only the isotope effect of translational and librational modes in the energy range $2 < E[\text{meV}] < 30$ (Figs. 9 and 10). Two equally strong peaks at 10.6 and 13.1 meV are the prominent feature of the spectrum. The energies of the other weak peaks

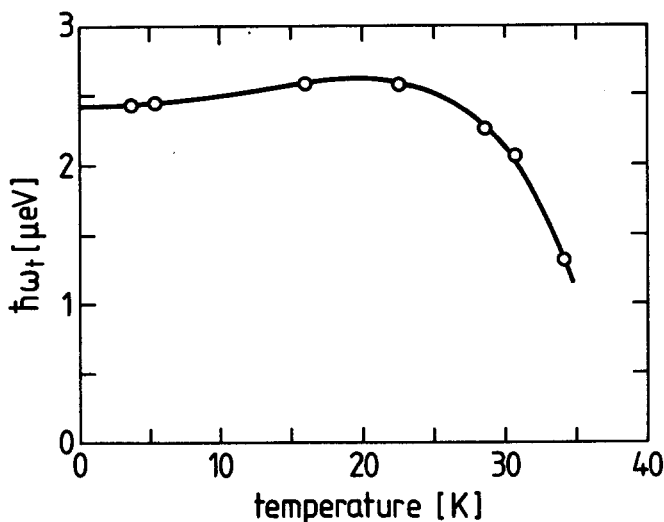


FIG. 7. Temperature dependence of the tunnel splitting $\hbar\omega_t$ in CH_3I . The solid line represents a fit with the model described in Sec. III A 5 using formula (12) and the parameters (13).

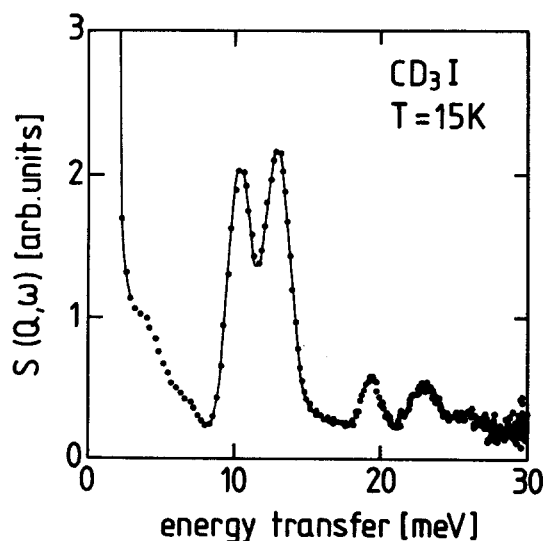
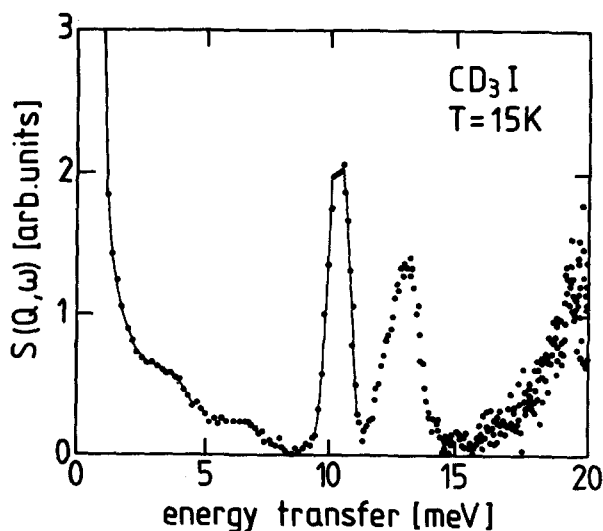


FIG. 9. As Fig. 2 but CD_3I .

FIG. 10. As Fig. 3 but CD_3I .

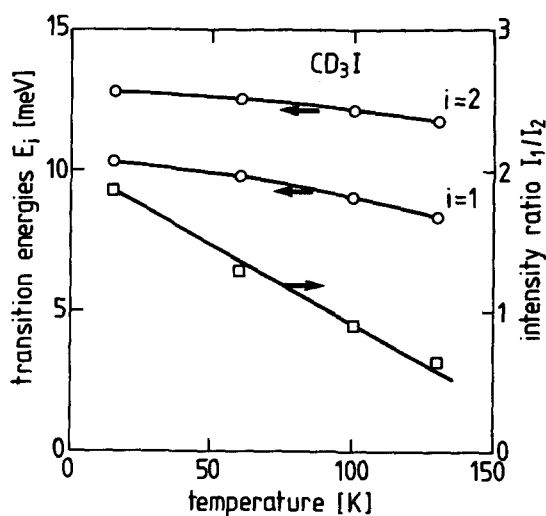
are given in Table III. For comparison, Raman and IR data from the literature²¹ are also presented. With increasing temperature the lower strong peak shifts considerably: At $T = 60$ K it is at 9.7 meV. At the same time it broadens significantly. The peak at 13.1 meV shifts less, being at 12.7 meV at $T = 60$ K, and broadens little. All these results are summarized in Fig. 11 which shows the line intensities and transition energies as a function of temperature.

3. CH_2DI

Only the methyl librations shift considerably with deuteration since their energy scales with the mass of the hydrogen atoms. All other modes scale with the mass of the whole molecule or parts of it. To follow more smoothly the isotope effect we have measured the excitations in the meV regime of one partially deuterated methyl iodide, as an intermediate case between CH_3I and CD_3I . The spectra are shown in Figs. 12 and 13. As expected we observe a doublet with peak energies of 11.84 and 13.5 meV. The peak at the higher energy

TABLE III. As Table I but for CD_3I .

$T = 18$ K	This work		Ref. 21	
	INS	60 K	Raman 20 K	Infrared 20 K
3.5			3.4	4.52
			4.2	
			6.0	
			6.3	
			7.6	7.06
6.7				
10.6 R_z		9.7	10.16 R_z	10.66
			12.02	
			12.76 R_x, R_y	12.52
13.1 R_x, R_y		12.7	12.95 R_x, R_y	13.51
			15.86	
19.5 R_z			18.96	
23.0			24.78	

FIG. 11. As Fig. 5 but CD_3I .

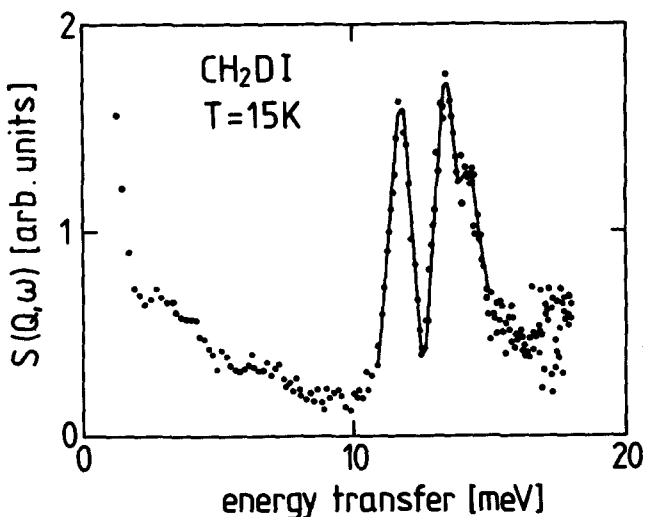
has a shoulder at 14.3 meV. All transition energies are tabulated in Table IV. With increasing temperature the peak at 11.84 meV is strongly damped (Fig. 13).

4. CH_3I in CD_3I

Since the tunneling splitting of the deuterated methyl group in CD_3I cannot be resolved by neutrons we lacked one important piece of information for an independent determination of the rotational potential of the methyl groups in CD_3I . To overcome this problem we used CH_3I as a probe in CD_3I .

Two samples were prepared which contained 2% and 50% CH_3I solved in CD_3I . Well-defined tunneling transitions were found. The transition energies are shifted compared to pure CH_3I . The tunnel splitting diminishes linearly with increasing concentration c_D of CD_3I (Fig. 14). An extrapolation to $c_D = 1$ yields a value $\hbar\omega_t = 2.02 \mu\text{eV}$.

The corresponding librational energies were determined with a sample containing 4% CH_3I in CD_3I . While the tun-

FIG. 12. As Fig. 3 but CH_2DI .

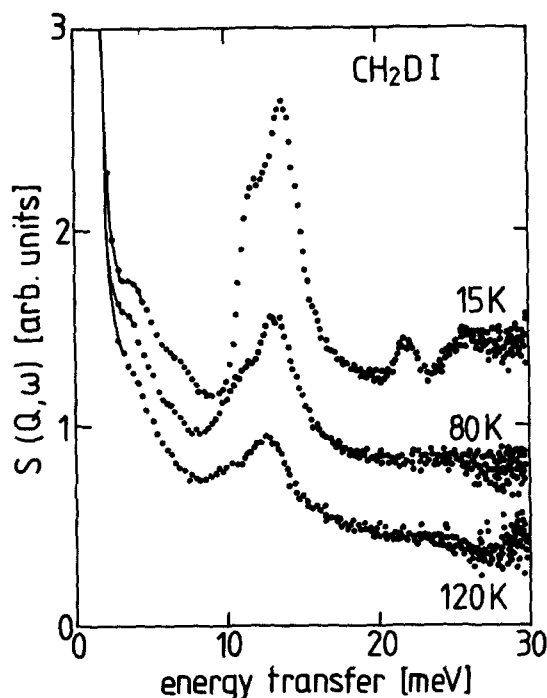


FIG. 13. Scattering function $S(Q, \omega)$ of CH_2DI as measured at the three indicated-sample temperatures to illustrate the change of the spectrum. An instrumental setup with an incident neutron wavelength $\lambda_0 = 1.51 \text{ \AA}$ was used. The other parameters as for Fig. 2.

neling transitions of the protonated and the deuterated methyl groups are far away from each other because of the strong isotope effect, the librational spectra overlap. At the chosen concentration (large enough to give a good signal from CH_3I but as low as possible) the contributions of CH_3I and CD_3I to the density of states are of the same order of magnitude. The resulting spectrum looks like a sum from Figs. 3 and 10. We show the spectrum only after subtraction of the CD_3I matrix (Fig. 15). Besides a shallow feature in the energy range $9 < E [\text{meV}] < 13$ which is due to an incomplete subtraction, there are two peaks left, a broad one at 13.8 meV and a very narrow line at 14.9 meV. In a wider energy range additional weak peaks are found at 25.1 and 28.4 meV.

B. Methyl bromide

1. CH_3Br

The principal features of CH_3Br are the same as for CH_3I . Figures 16 to 18 show the spectra in the meV regime.

TABLE IV. As Table I but for CH_2DI and without a reference.

This work	
$T = 15 \text{ K}$	40 K
3.0	
3.8	
6.4	
11.84 R_z	11.7
13.5 R_x, R_y	13.3
14.3 R_x, R_y	14.3

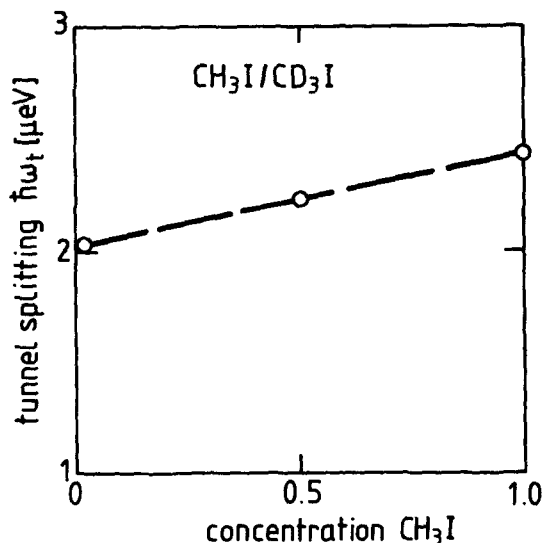


FIG. 14. Ground state tunnel splitting of the methyl group of CH_3I in mixtures $\text{CH}_3\text{I}/\text{CD}_3\text{I}$ as measured at sample temperatures $T = 5 \text{ K}$. The splitting decreases linearly by going from pure CH_3I to nearly pure CD_3I .

The peak positions are given in Table V. Literature values of Raman and IR spectra²⁰ are also presented for comparison. The lines only shift slightly when the temperature is increased to $T = 36 \text{ K}$.

The high resolution spectrum was recorded only at one temperature, $T = 5 \text{ K}$ (Fig. 19), and shows a tunneling transition at $\hbar\omega_t = 0.9 \mu\text{eV}$.

Before melting CH_3Br undergoes a solid–solid phase transition.^{2,20} We have measured the density of states for various temperatures around the transition point (Fig. 20). At these high temperatures the spectra look rather smooth and the features are little pronounced. However, it is clearly seen, that in the intermediate phase a second peak has evolved at higher energy transfer 16.0 meV. This peak is still found in the liquid, while at low temperatures $T < 170 \text{ K}$ only one broad line exists at about 13 meV. This line contains the unresolved and shifted doublet of Fig. 17.

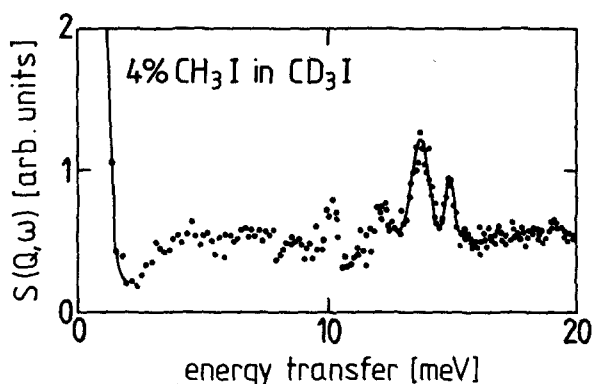
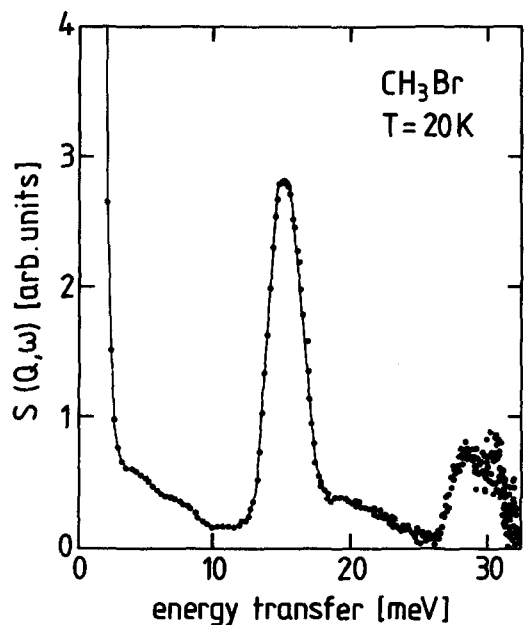


FIG. 15. Scattering function $S(Q, \omega)$ of CH_3I impurities in a matrix of CD_3I . The spectrum is obtained by subtracting the CD_3I matrix spectrum from the measured spectrum of the mixed system. The instrumental setup was as in Fig. 3.

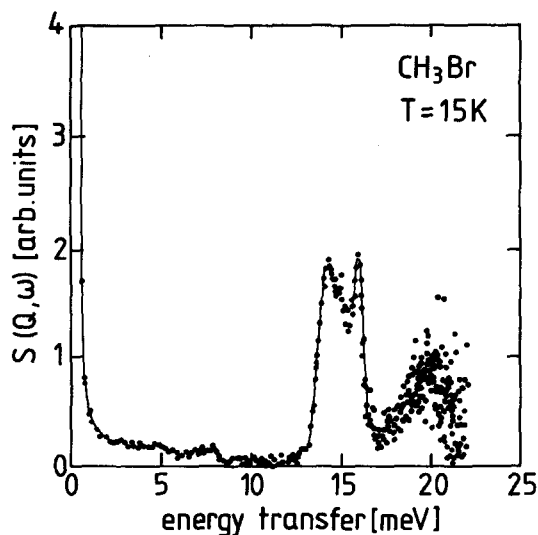
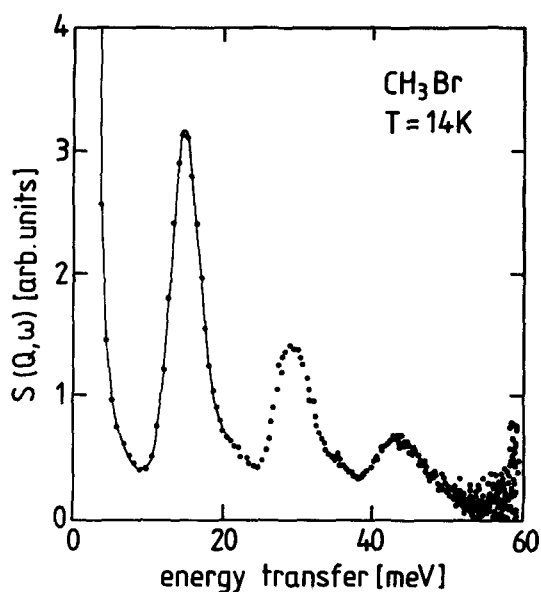
FIG. 16. As Fig. 2 but CH_3Br .

2. CD_3Br

Spectra of the deuterated material were taken in the energy range $2 < E$ [meV] < 30 using two setups of the spectrometer SV22 (Figs. 21 and 22) and at two different temperatures. There is again a dominating doublet line and less pronounced peaks at about twice their energy. The transition energies are shown in Table VI together with the most recent Raman and IR results from the literature.²⁰

C. Methyl chloride CH_3Cl

Despite the different structure, the inelastic spectra of CH_3Cl look quite similar to those of CH_3Br and CH_3I . For the various energy regions the spectra are shown in Figs. 23 and 24 and the derived mode frequencies are summarized in Table VII together with literature values from Raman and

FIG. 17. As Fig. 3 but CH_3Br .FIG. 18. As Fig. 4 but CH_3Br .

infrared measurements.²² Besides some weak peaks below 10 meV we again observe an intense doublet line now at energy transfers 15.4 and 18.1 meV, the latter having an internal structure. With increasing temperature the peak at 18.1 meV decreases rapidly in intensity and shifts to smaller energies (cf. Table VII).

III. DISCUSSION

We have obtained the most detailed data from methyl iodide. Thus we will concentrate our initial discussion on this compound and use the results for the interpretation of the similar spectra from methyl bromide. Emphasis here will

TABLE V. As Table I but for CH_3Br and Ref. 20.

This work		Ref. 20	
$T = 18 \text{ K}$	INS 36 K	Raman 20 K	Infrared 20 K
4.8		4.96	5.45
		5.76	
		7.25	
		7.68	
7.9	7.6	7.74	8.18
		8.55	
14.2 R_x, R_y	14.2	13.94 R_x, R_y	
14.8 R_x, R_y	14.6	14.50 R_x, R_y	14.44
15.8 R_z	15.7	14.99 R_x, R_y	15.37
		15.24 R_z	16.48
		18.58	18.84
19.5		21.56	21.44
		27.51	
28.8 R_z		29.37	
43.0			

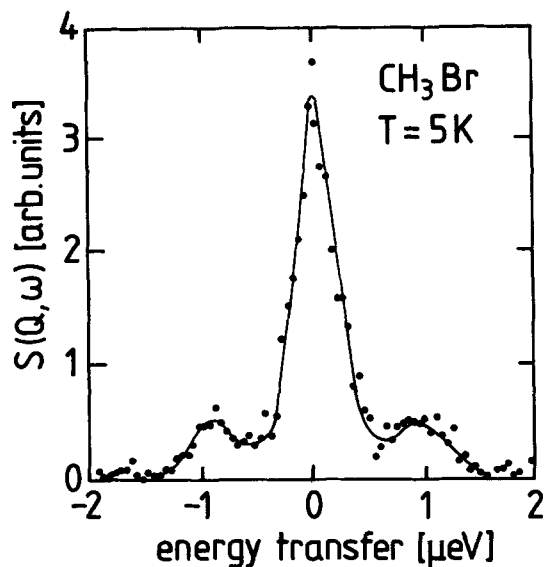


FIG. 19. As Fig. 6 but CH_3Br and $\hbar\omega_{\text{tun}} = 0.9 \mu\text{eV}$.

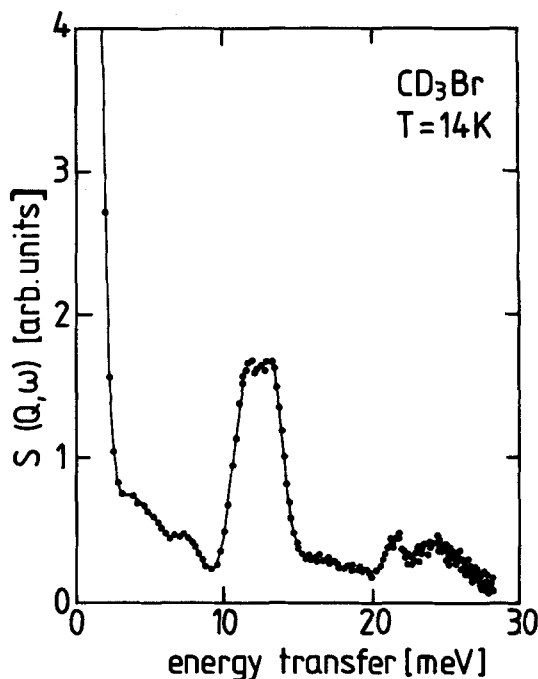


FIG. 21. As Fig. 2 for CD_3Br .

be given only to the different features. The spectra from methyl chloride are used for a comparison with the β -phase of methyl bromide.

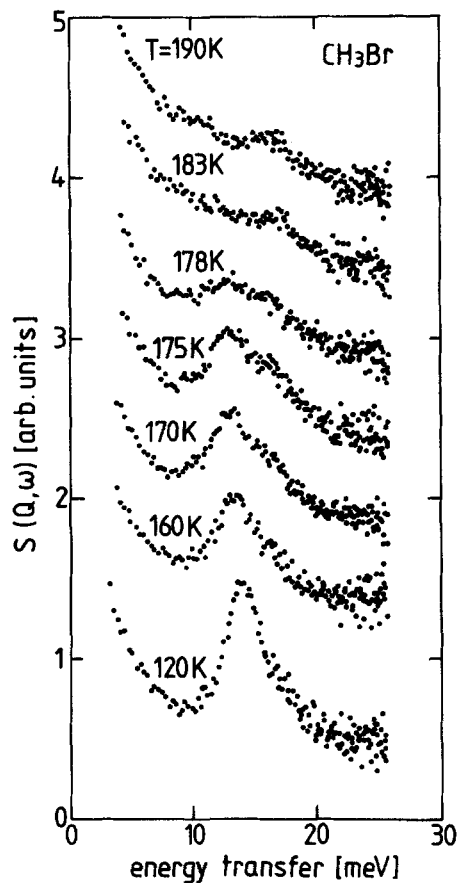


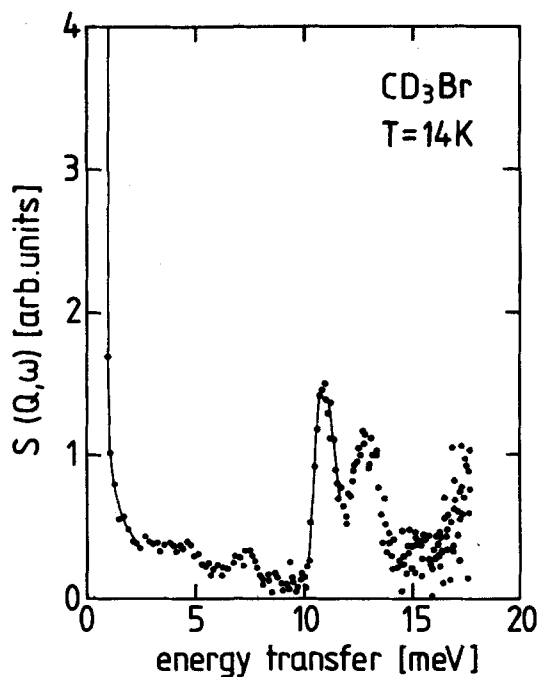
FIG. 20. Scattering function $S(Q, \omega)$ of CH_3Br in the meV region and at temperatures covering β - CH_3Br ($T < 174 \text{ K}$), the α -phase ($174 < T < 178 \text{ K}$) and liquid CH_3Br ($T > T_m = 178 \text{ K}$). The instrumental setup was as for Fig. 2.

A. Methyl iodide

As a consequence of the structure,¹ all methyl groups in solid methyl iodide are equivalent. The relative intensity of the tunneling line at $Q = 1.40 \text{ \AA}^{-1}$ is in agreement with the theoretically predicted value²⁶ while the intensity ratio at $Q = 1.88 \text{ \AA}^{-1}$ cannot be evaluated due to a contamination of the elastic intensity by Bragg reflection.

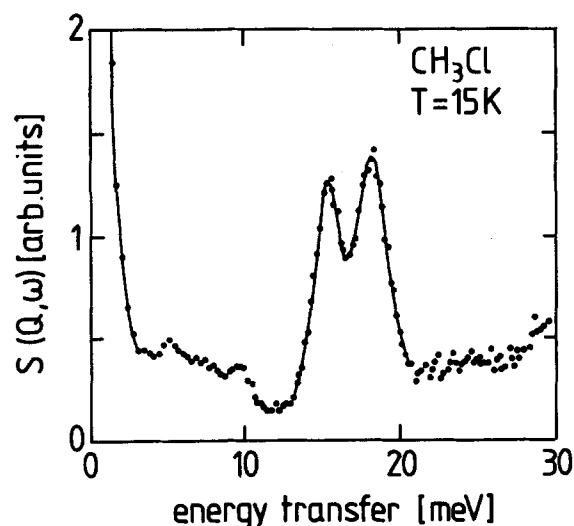
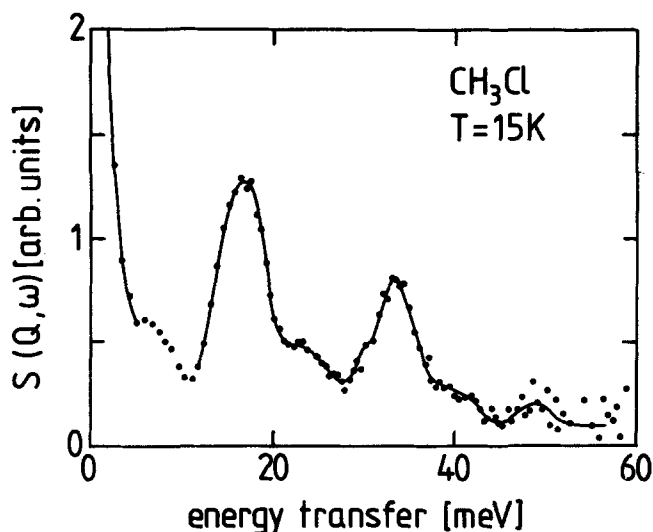
TABLE VI. As Table IV but for CD_3Br and Ref. 20.

	This work		Ref. 20	
	INS	42 K	Raman 20 K	Infrared 20 K
$T = 15 \text{ K}$				
4.5			4.89	5.39
			5.70	
			7.13	
7.4			7.62	
			7.74	
			8.43	8.05
11.1 R_z		11.0	10.90 R_z	11.52
12.8 R_x, R_y		12.8	12.45 R_x, R_y	
13.2 R_x, R_y			13.07 R_x, R_y	13.25
			13.51 R_x, R_y	
				14.56
				17.72
21.5			21.19	20.45
24.1			25.28	

FIG. 22. As Fig. 3 for CD_3Br .

1. Coupling of tunnelling rotors

Before the measurements of deuterated species of methyl iodide were finished we considered orientational coupling to be the reason for the observed doublets in the meV spectra Fig. 3. The crystallographic structure of CH_3I suggest this interpretation. In a model, only considering the proton-proton interaction of Dows¹² $V(r) = A e^{-Br}$, $A = 1.2 \times 10^{-10}$ erg, $B = 3.52 \times 10^8 \text{ cm}^{-1}$ and using x-ray diffraction data for the equilibrium atom positions from Ref. 1 we have estimated the coupling strength along the crystallographic a and b axis. As a result we find that the coupling in the a direction is four times as strong as in the b direction. The exact numerical values, however, depend on the chosen proton-proton potential but a more sophisticated potential as in

FIG. 23. As Fig. 2 but CH_3Cl .FIG. 24. As Fig. 4 but CH_3Cl .

Ref. 15 leads to rather similar values. These considerations led us to the assumption of one dimensional chains of coupled rotors. In the harmonic approximation and for weak coupling we expect for the density of the librational states a symmetric splitting Γ_{01} proportional to the coupling strength W_3 . We estimate the strength of such a coupling from Fig. 3 and use the model of the coupled methyl rotors²⁷ as a very short one-dimensional chain. With $W_3/V_3 = \Gamma_{01}/E_{01}$, V_3 being the single particle potential and E_{01} the average energy of the first excited librational state, Figs. 4 and 5 of Ref. 27 reflect an expected broadening of the tunneling line of less than 1%. We see that the librational spectrum might indicate orientational coupling with very strong potentials better than tunneling, at least in the case of a low dimensional system. However, the two components of the observed doublet show a very different shift and broadening with temperature and thus cannot come from the same mode. Because of the faster broadening with temperature and the isotope effects (see below) we identify only the transition at 13.7 meV as a libration. Thus coupling effects might only show up in a line broadening of this transition which is found

TABLE VII. As Table I but for CH_3Cl and Ref. 22.

This work		Ref. 22		
$T = 10 \text{ K}$	INS	$T = 82 \text{ K}$	Raman	Infrared
			$T = 20 \text{ K}$	
			7.8	
			8.9	8.9
			10.7	10.7
			15.1	
15.4 R_x, R_y		14.8	15.5	15.5
			16.2 R_x, R_y	16.2
			17.5	16.7
18.1 R_z		16.9		
			19.2	
			20.2 R_z	20.2

to be less than 0.15 meV or below 1% of the single particle excitation around the molecular axis.

In the following we now describe the rotational potential of the methyl group as a single particle rotational potential.

2. Single particle rotational potential

Because we cannot explain $\hbar\omega_i$ and E_{01} in terms of a simple Mathieu problem we take into account higher order Fourier components of the rotational potential

$$V(\varphi) = \frac{V_3}{2} [1 + (-1)^k \cos 3\varphi] + \frac{V_6}{2} [1 + (-1)^k \cos 6\varphi]. \quad (4)$$

The corresponding eigenvalues are tabulated²⁸ or can easily be calculated. Using two transition energies, namely the tunnel splitting $\hbar\omega_i = 2.44 \mu\text{eV}$ and the librational energy $E_{01} = 13.27 \text{ meV}$, we can fix the two parameters V_3 and V_6 . We get one solution for each value of $k = 0, 1$. It is more convenient to characterize the potential by $VS = V_3 + V_6$, the total strength of the potential, and $\delta = V_3/VS$, the contribution of a pure $\cos 3\varphi$ potential. We get

$$k = 0, \quad \frac{1}{2} VS = 24.9 \text{ meV}, \quad \delta = 0.92, \quad (5)$$

$$k = 1, \quad \frac{1}{2} VS = 25.5 \text{ meV}, \quad \delta = 0.265. \quad (6)$$

The solution (5) represents a potential with a narrowed barrier between the equilibrium orientations. The deviation from the pure $\cos 3\varphi$ potential is small. The solution (6) gives a dominant sixfold potential and the barriers between the minima are strongly broadened. Both potentials give energies for a second excited librational state in the same range, namely at $E_{02} = 24.6$ and 23.4 meV for Eqs. (5) and (6), respectively. Indeed we find a weak peak at 24.2 meV which shows a temperature dependence similar to E_{01} . We will show below (Sec. III A 3) that on the basis of the isotope effect we can reject the solution (6). Thus in accordance with a general systematic^{29,30} the single particle potential in methyl iodide is close to a threefold cosine potential.

The second strong peak at an energy 14.54 meV we assign to librations R_x, R_y ¹⁵ about axes perpendicular to the symmetry axis of the molecular. Such a motion is found in the same energy range in a recent Raman and IR study.²¹ Since it involves a large amplitude motion of the hydrogen atoms it appears as a strong line in the inelastic neutron spectra.

3. Isotope effects

The isotope effect can be used to identify the type of motion related with a peak in the density of states. Two assumptions are made: (i) the crystal structure is unchanged by deuteration so the effect is a pure mass effect, (ii) the potentials are harmonic. Under these conditions we will observe an isotope effect of about $(m_1/m_2)^{1/2}$ for acoustic modes, $(m_{m1}/m_{m2})^{1/2}$ for librations perpendicular to the molecular symmetry axis, and $(\theta_1/\theta_2)^{1/2}$ for the methyl librations. Here m_i is the mass of the whole molecule, m_{mi} that of the methyl group, and θ_i its momentum of inertia.

TABLE VIII. Comparison of librational frequencies and isotopic ratio $\Delta^{\text{isotop}} = E_{01}^{\text{prot}}/E_{01}^{\text{deut}}$ for systems with equal ground state tunnel splitting.

	Single particle potential (5)	From Eq. (11) with parameters (13)	Observed in CH_3I
E_{01}^{prot} [meV]	13.27	13.86	13.27
Δ^{isotop}	1.36	1.35	1.252

The methyl librations are most strongly affected by deuteration. However, the rotational potential is not harmonic [assumption (ii)] and this will reduce the isotope effect somewhat: not the excitation energy but the potential has to be scaled with respect to the new masses. If we make a mode assignment as suggested by the temperature dependence of the various peaks in the density of states and as shown in Tables I, III, and IV we find an isotope shift of nearly the expected order of magnitude for the R_x, R_y modes at 14.54 meV , $(16/15)^{1/2}$ for CH_2DI and $(18/15)^{1/2}$ for CD_3I , but a strongly reduced isotope effect for the methyl libration R_z at 13.27 meV . Table VIII shows the effect expected by scaling the potential (5) and the observed one. A formal attempt to use the 14.54 meV mode in CH_3I as a methyl libration—which is inconsistent with the observed temperature effects—leads to an isotopic shift of the assigned R_x, R_y modes in the wrong direction, which makes no sense. Thus we are sure that our assignment is correct. The fact, that the observed isotopic shift is smaller than expected, means that the rotational potential in the deuterated material has considerably increased.

Since in the deuterated derivatives the R_z and R_x, R_y modes are energetically better resolved, we can observe a fine structure of the R_x, R_y line which could not be seen in the spectrum of the fully protonated material because it is partially hidden by the overlapping methyl libration. This splitting most probably is a consequence of the low site symmetry, which makes the hindering potential of the librations around the two orthogonal axis perpendicular to the molecular symmetry axis (x and y direction) different.

Due to its temperature dependence and to the fact that their relative isotopic shift is identical to E_{01} we interpret the peak at 24.2 (CH_3I), 22.0 (CH_2DI), and 19.5 (CD_3I) meV as the second librational excitation. With this assignment we are in disagreement with the eigenenergies calculated for the potential (6) and thus can reject this solution.

The most astonishing observation is the existence of a large isotopic effect beyond the simple mass effect, which cannot be described by any of our models (Table VIII and see Sec. III A 5 where the coupling phonons is discussed). To determine the size of this effect quantitatively we have been using CH_3I as a probe in CD_3I . The librational peak has shifted now to $E_{01} = 13.8 \text{ meV}$. It shows a width which might be the result of the disorder. The shift of the librational transition to larger energies is combined with a considerable reduction of the tunnel splitting. From these two excitations we again derive a rotational potential. Since we have excluded the case $k = 1$ we show only the solution

$$k = 0, \quad \frac{1}{2}VS = 26.2 \text{ meV}, \quad \delta = 0.92. \quad (7)$$

While the shape of the potential is almost unchanged in the CD_3I matrix its strength is increased by about 5%.

For CD_3I we find on the basis of $E_{01} = 10.6 \text{ meV}$ and keeping the potential shape fixed parameters

$$k = 0, \quad \frac{1}{2}VS = 29.5 \text{ meV}, \quad \delta = 0.92. \quad (8)$$

Thus the rotational potential has further increased in the fully deuterated material. The more localized deuterated methyl groups obviously interact more strongly with their surrounding. A change of the rotational potential with deuteration as in methyl iodide is rarely observed with other compounds.

In the partially deuterated CH_2DI we can derive a rotational potential from the first excited librational level $E_{01} = 11.8 \text{ meV}$ only. The additional assumption that the potential shape is similar to that in the fully protonated material is justified by the dilution experiment. We get

$$k = 0, \quad \frac{1}{2}VS = 25.8 \text{ meV}, \quad \delta = 0.92. \quad (9)$$

Thus the above considerations show that rather unexpectedly²¹ the increasing deuteration has a tremendous effect on the strength of the rotational potential: in the partially deuterated material there is a slight increase in the single particle potential height of about 4% compared to the protonated sample. But full deuteration leads to the remarkable increase of about 25% in the rotational barrier which might have its reason in a new equilibrium inclination of the molecular axis in the a - c plane. The tunnel splitting of the CD_3 group in the potential (8) would be $\hbar\omega_t = 6.5 \text{ neV}$ (1.56 MHz).

4. Comparison with other experimental results

Our interpretation of the data is in slight disagreement with the assignment of modes given in a recent study of methyl iodide using Raman and IR spectroscopy.²¹ According to this paper the methyl libration in CH_3I should be above 14 meV. The interpretation of the CD_3I spectra, however, agrees with ours.

From a NMR- T_1 curve of CH_3I , which is characteristic of a relaxation of tunneling methyl groups,^{1,32} one derives³³ the same values for E_a , E_{01} , and consistent ones for $\hbar\omega$, as we have found with our assignment. In a quasielastic neutron scattering experiment, however, a somewhat smaller activation energy E_a for classical reorientation is observed for CD_3I .³⁴

5. Temperature dependence of the tunnel splitting

While the low temperature tunneling spectrum of CH_3I does not show special features, their temperature dependence is rather peculiar (Fig. 7). With rising temperature it first increases by about 6% before it moves towards smaller energies as is usually observed.²⁶ Recently, a few other examples have been found with a similar temperature dependence, e.g., $\text{Pb}(\text{CH}_3)_4$,³⁵ $(\text{NH}_4)_2\text{SnBr}_6$,³⁶ or $(\text{NH}_4)_2\text{ZnCl}_4$.³⁷ We do not believe that the thermal expansion is responsible for the increasing tunnel splitting at low temperatures as proposed in Ref. 37. In CH_3I it could be that the orientation of the molecule changes somewhat with temperature since the inclination with respect to the c axis is a free parameter of the structure. A rotation by less than 1°

would be sufficient to explain the observed effect. Temperature dependent diffraction studies are planned to check this possibility. A similar interpretation is difficult in the other examples³⁵⁻³⁷ where the molecular orientation is defined by symmetry. Thus we believe that the increase of the tunnel splitting with increasing temperature could be a fundamental feature of the coupling of a tunneling rotor to low frequency phonons which modulate the single particle potential rather than distort it. As has been emphasized before, orientational hindering due to intramolecular forces is absent in CH_3I and so we expect a pronounced coupling of the methyl orientation to intermolecular degrees of freedom. For the relevant Hamiltonian we assume

$$\begin{aligned} H &= H^{\text{Rot}} + H^{\text{Phon}} + H^{\text{Int}}, \\ H^{\text{Rot}} &= \frac{L_\varphi^2}{2\theta} + V_3 \cos 3\varphi, \\ H^{\text{Phon}} &= \sum_k \left\{ \frac{P_k^2}{2m_k} + \frac{m_k}{2} \omega_k^2 x_k^2 \right\}, \\ H^{\text{Int}} &= H^c + H^s, \\ H^c &= \sum_k \left(\frac{2m_k \omega_k}{\hbar} \right)^{1/2} g_k^c x_k \cos 3\varphi, \\ H^s &= \sum_k \left(\frac{2m_k \omega_k}{\hbar} \right)^{1/2} g_k^s x_k \sin 3\varphi. \end{aligned} \quad (10)$$

As will be shown in a forthcoming paper,³⁸ for the coupling of a methyl rotor to a single oscillator mode, the two components H^c and H^s of H^{Int} may lead to an opposite temperature dependence within the physically reasonable range for V_3 , ω_k , and $g_k^{c,s}$. This qualitative remark is in full agreement with Hewson's second order perturbation theory.⁷

Thus if we neglect fourth order terms in a perturbation expansion with respect to H^{Int} we can distinguish between the effect of H^s leading to the well-known decrease of the tunneling frequency with increasing temperature³⁹ and the effect of H^c which rather enhances the tunneling frequency with an increase in the phonon population. A lattice dynamics calculation should confirm this coupling of the form $x_k \cdot \cos 3\varphi$ to phonon modes, which in CH_3I must have low energies to become effective at the low temperatures, while a coupling of the form $x_k \cdot \sin 3\varphi$ to high energy modes causes the decrease of $\hbar\omega_t$ above 20 K.

If we are interested in a more quantitative description of the shift of the tunneling line at low temperature we may simulate the phonons by a dispersionless Einstein mode and consider the following simplified Hamiltonian:

$$\begin{aligned} H &= \frac{L_\varphi^2}{2\theta} + V_3 \cos 3\varphi + \frac{P^2}{2m} + \frac{m}{2} \omega^2 x^2 \\ &+ g^c \sqrt{\frac{2m\omega}{\hbar}} x \cos 3\varphi. \end{aligned} \quad (11)$$

This Hamiltonian has the property that there is a temperature dependent equilibrium value for the oscillator position. We can calculate the eigenvalues of Eq. (11) numerically³⁸ and it turns out that the tunneling frequencies corresponding to two adjacent oscillator levels n and $n+1$ have approximately a constant ratio $\hbar\omega(n+1)/\hbar\omega(n) = 1 + A^c$.

So we may represent the temperature dependent value of $\hbar\omega_i(T)$ as a superposition of two contributions:

$$\hbar\omega_i(T) = \hbar\omega_i(0) \left\{ \frac{1 - \exp(-E^c/k_B T)}{1 - (1 + A^c)\exp(-E^c/k_B T)} - A^s \exp(-E^s/k_B T) \right\} \quad (12)$$

Here the decrease of the tunnel splitting occurring at high temperatures is described by a simple Arrhenius behavior.

From the observed data (Table II) we did look for the best activation energies $E^{c,s}$ and prefactors $A^{c,s}$ which are:

$$\begin{aligned} A^c &= 0.220, & E^c &= 2.15 \text{ meV}, \\ A^s &= 49.06, & E^s &= 12.94 \text{ meV}, \end{aligned} \quad (13)$$

and we can find suitable parameters V_3 , $\hbar\omega$, and g^c describing the increasing contribution to $\hbar\omega_i(T)$ in Eq. (12):

$$V_3 = 18.2 \text{ meV}, \quad \hbar\omega = 2.15 \text{ meV}, \quad g^c = 2.9 \text{ meV}. \quad (14)$$

With this choice of parameters we get the solid line in Fig. 7 which is an excellent description of the data and we calculate a librational energy from Eq. (11) of 13.86 meV which is somewhat higher than observed (cf. Tables I and VIII). In the above model we cannot discuss nor exclude a contribution to the single particle orientational potential of sixfold symmetry.

We can calculate the shift of the first excited librational state with deuteration in the framework of the presented model, which has shown the importance of the coupling to phonons. If we scale only the rotational part of the Hamiltonian by simple replacing the rotational constant of the methyl group B_H by $B_D = B_H/2$ we find an isotopic shift by a factor $\Delta^{\text{isotop}} = E_{01}^{\text{prot}}/E_{01}^{\text{deut}} = 1.35$ which is considerably larger than the observed one $\Delta^{\text{isotop}} = 1.25$. Additionally, we can take into account a change of the oscillator frequency and of the coupling strength due to the enlarged translational mass m of the methyl group. It was expected that such a scaling would explain the large isotope effect observed. However, the additional reduction of the isotopic ratio Δ^{isotop} calculated was, for all possible cases (coupling via H^c or H^s , different scaling of m), rather small with a minimal value $\Delta_{\text{min}}^{\text{isotop}} \approx 1.32$.

B. Methyl bromide

The experiments performed with methyl bromide are not as detailed as those with methyl iodide. Since the two materials show the same low temperature structure we can, however, profit from our previous data analysis of methyl iodide.

1. Coupling of tunneling rotors

Due to the reduced interatomic distances in CH_3Br compared to CH_3I we expect an increasing importance of orientational coupling (being an octupole–octupole interaction). But even this stronger coupling does not lead to an observable linewidth of the librational peak at 15.8 meV (see below).

2. Single particle rotational potential

In agreement with the expectation of an increased single particle potential compared to CH_3I we find a smaller tunnel splitting ($\hbar\omega_i = 0.9 \mu\text{eV}$) and a larger librational energy ($E_{01} = 15.8 \text{ meV}$). The identification of E_{01} is done on the basis of the stronger temperature dependence of the peak and via the isotope effect (see Sec. III B 3). From these two eigenenergies we obtain a purely threefold cosine potential ($\delta = 1$) of a strength $V_S = 52.4 \text{ meV}$.

The second excited librational state in this potential appears at an energy $E_{02}^{\text{cal}} = 29.6 \text{ meV}$ which is close to the measured value $E_{02} = 28.8 \text{ meV}$.

3. Isotope effects

We know from methyl iodide that the R_x , R_y modes shift by full deuteration by a factor close to $(18/15)^{1/2}$. The same factor is found to relate the peak at 14.2/14.8 meV in CH_3Br with that at 12.8/13.2 meV in CD_3Br . As in methyl iodide the R_x , R_y modes are doublets. The origin of this splitting again is the low symmetry of the surrounding.

These peaks also are less influenced by increasing temperature than the remaining second strong peak at 15.8 meV in CH_3Br and at 11.1 meV in CD_3Br . These transitions are therefore assigned to the methyl libration. The ratio of the transition energies is close to $\sqrt{2}$, a factor which is also nearly reproduced by scaling the rotational potential (15) for the deuterated material ($E_{01}^{\text{cal}} = 11.5 \text{ meV}$). The energy of the second excited librational state is calculated to be $E_{02}^{\text{cal}} = 22.1 \text{ meV}$ and found at $E_{02} = 21.5 \text{ meV}$. The tunnel splitting in CD_3Br in the proposed rotational potential (15) is $\hbar\omega_i = 5.5 \text{ neV}$ or 1.32 MHz. Thus in contrast to methyl iodide the isotope effect in methyl bromide is fully explained by the scaling of the masses. The above assignment is fully consistent with the interpretation of the recent Raman and IR study.²⁰

4. Phase transition

At $T_c = 173.75 \text{ K}$ CH_3Br undergoes a solid–solid phase transition from the low temperature β -phase to the high temperature α -phase which has the same structure as CH_3Cl .² This would mean that at the phase transition each second molecule in the chain along the c direction makes a 180° flip. The new head to tail arrangement of the molecules should give rise to a change of the rotational potential which will show up in the density of states. Indeed, besides the low temperature line shifted with increasing temperature to 12.7 meV a new peak at about 16 meV is observed. Since the methyl librations are already strongly damped at these temperatures we believe that the two peaks represent the two eigenmodes of the R_x , R_y libration. The new broad peak at 16 meV survives if the sample is liquified. Because of the isotropic surrounding in the liquid the R_x and R_y modes now are degenerate.

C. Methyl chloride

It is most astonishing that the spectra of CH_3Cl are rather similar to those of the two other measured methyl halides (CH_3I and CH_3Br) at low temperature. All modes seem to

be shifted to higher energies. From its temperature dependence the peak at 18.1 meV is assigned to the methyl libration. A purely threefold cosine potential derived therefrom has a strength $V_3 = 66$ meV. The peak at 15.4 meV is then most probably due to a libration perpendicular to the molecular axis. On the basis of the different crystal structures^{1,4} a more drastic change of the inelastic spectrum was expected. Having in mind that CH_3F is assumed to solidify in the same structure as CH_3Br and CH_3I ⁴⁰ we may ask the question whether the structure of CH_3Cl , being a member in this sequence of methyl halides, is really different from that of the others.⁴¹

IV. SUMMARY AND CONCLUSIONS

The single particle rotational behavior of methyl groups in methyl iodide, bromide, and chloride has been investigated using the inelastic incoherent neutron scattering technique. The doublet line found in the density of states is suggestive of a rotor-rotor coupling of the methyl groups but such a coupling can be excluded because of the different temperature dependence and isotope effects of the two sublimes. One transition is due to the methyl libration and the other, split because of the low site symmetry, to molecular librations around axes perpendicular to the carbon-halogen bond axis.

Single particle rotational potentials have been determined for CH_3I , CH_3Br in CD_3I and CH_3Br from the transition energy to the first excited librational state and the tunnel splitting. Under the assumption of unchanged shape—confirmed for CH_3I in CD_3I experimentally—potentials were also obtained for the deuterated materials. While the potential strength in the bromide is not affected by deuteration—the isotope effect is fully explained by a scaling of the masses—we find a strong increase of the rotational potential with deuteration in methyl iodide. This leads to a largely reduced shift of the librational modes by deuteration and is probably the reason for a wrong assignment in a recent Raman and FIR study of methyl iodide.²¹

The temperature dependence of the tunnel splitting is a consequence of a coupling of the methyl rotor to the phonons which rather modulate the single particle potential than distort it. The astonishing shift to larger energies in CH_3I (also established for CH_3I in CD_3I) is explained by a coupling of the methyl rotation to an Einstein oscillator via an interaction Hamiltonian $H^c \sim x \cdot \cos 3\varphi$ not considered so far. The well-known shift to lower energies at higher temperatures was taken into account phenomenologically. The description yields reasonable parameters.

Much more complete information on the molecular dynamics could be achieved by measuring the dispersion curves by inelastic coherent neutron scattering in a deuterated single crystal. Such data should support our above interpretations and help to clarify open questions. It would also stimulate theoretical efforts in determining the intermolecular potentials in the methyl halides with a full lattice dynamical calculation. The much simpler experiment reported here, however, has already given very interesting results going beyond those obtained by other techniques.

ACKNOWLEDGMENTS

We thank A. Heidemann for the support with the experiment in Grenoble, G. Eckold and especially M. Monkenbusch for performing lattice dynamical calculations and F. Joswig for his help with the experiments in Jülich. One of us (W. H.) wants to thank A. Hüller for helpful discussions about many details concerning this paper.

¹T. Kawaguchi, M. Hijikigawa, Y. Hayaftiyi, M. Ikeda, R. Fukushima, and Y. Tomie, *Bull. Chem. Soc. Jpn.* **46**, 53 (1973).

²P. N. Gerlach, B. H. Torrie, and B. M. Powell, *Mol. Phys.* **57**, 919 (1986).

³L. W. G. Wyckoff, *Crystal Structures* (Wiley, New York, 1964), Vol. 1, p. 52.

⁴R. D. Burbank, *J. Am. Chem. Soc.* **75**, 1211 (1953).

⁵S. Clough, A. Heidemann, A. H. Horsewill, and M. N. J. Paley, *Z. Phys. B* **55**, 1 (1984).

⁶M. Prager, A. Heidemann, and W. Häusler, *Z. Phys. B* **64**, 447 (1986).

⁷A. C. Hewson, *J. Phys. C* **15**, 3841, 3855 (1982).

⁸S. Clough, A. Heidemann, and M. Paley, *J. Phys. C* **12**, 1001 (1981).

⁹P. Brüesch, *Phonons: Theory and Experiments I*, Springer Series in Solid State Sciences Vol. 34 (Springer, Berlin, 1982).

¹⁰K. H. Link, H. Grimm, B. Dorner, H. Zimmermann, H. Stiller, and P. Bleckmann, *J. Phys. Chem. Solids* **46**, 135 (1985).

¹¹Z. Gamba and H. Bonadeo, *J. Chem. Phys.* **75**, 5059 (1981).

¹²D. A. Dows, *J. Chem. Phys.* **29**, 484 (1958); **33**, 1743 (1960).

¹³M. E. Jacox and R. M. Hexter, *J. Chem. Phys.* **35**, 183 (1960).

¹⁴W. L. Lafferty and D. W. Robinson, *J. Chem. Phys.* **36**, 83 (1962).

¹⁵J. Takeuchi, J. L. Bribes, I. Hirada, and T. Shimanouchi, *Bull. Chem. Soc. Jpn.* **49**, 3843 (1976).

¹⁶M. Ito, *J. Chem. Phys.* **41**, 2842 (1964).

¹⁷C. W. Brown and E. R. Lippincott, *J. Chem. Phys.* **52**, 786 (1970).

¹⁸H. Takeuchi, J. L. Bribes, I. Hirada, and T. Shimanouchi, *J. Raman Spectrosc.* **4**, 235 (1976).

¹⁹J. A. Janik, A. Bajorek, J. M. Janik, I. Natkaniec, K. Parlinski, and M. Sudnik, *Acta Phys. Pol.* **XXXIII**, 419 (1968).

²⁰O. S. Binbrek, A. Anderson, and B. H. Torrie, *J. Chem. Phys.* **82**, 1468 (1985).

²¹O. S. Binbrek, A. Anderson, B. Andrews, and B. H. Torrie, *J. Raman Spectrosc.* **15**, 406 (1984).

²²A. Anderson, B. Andrews, and B. H. Torrie, *J. Chim. Phys. (Paris)* **82**, 99 (1985).

²³M. Prager, K. H. Duprée, and W. Müller-Warmuth, *Z. Phys. B* **51**, 309 (1983).

²⁴B. Maier, Neutron facilities at the HFR Grenoble 1984, Copies may be obtained from the Scientific Secretary, ILL, 156 X, F-38042 Grenoble Cedex.

²⁵H. Pohl and M. Prager, Internal Report JÜL-SPEZ-176 (1982).

²⁶W. Press, *Title*, Springer Tracts in Modern Physics, Vol. 92 (Springer, Berlin, 1981).

²⁷W. Häusler and A. Hüller, *Z. Phys. B* **59**, 177 (1985).

²⁸R. F. Gloden, *Euratom Reports* EUR 4349 and EUR 4358 (1970).

²⁹S. Clough, A. Heidemann, A. J. Horsewill, J. D. Lewis, and M. N. J. Paley, *J. Phys. C* **14**, L525 (1981).

³⁰W. Müller-Warmuth, K. H. Duprée, and M. Prager, *Z. Naturforsch. Teil A* **39**, 66 (1983).

³¹J. Haupt, *Z. Naturforsch. Teil A* **26**, 1578 (1971).

³²W. Müller-Warmuth, R. Schüler, M. Prager, and A. Kollmar, *J. Chem. Phys.* **69**, 2382 (1978).

³³W. Müller-Warmuth (to be published).

³⁴S. Clough and D. Cavagnat, ILL report 9-03-406 (1984).

³⁵M. Prager and W. Müller-Warmuth, *Z. Naturforsch. Teil A* **39**, 1187 (1984).

³⁶L. P. Ingman, M. Punkkinen, E. E. Ylinen, and C. Dimitropoulos, *Proc. 17th Annu. Conf. Finnish Phys. Soc.* **7**, 20 (1983).

³⁷L. P. Ingman, M. Punkkinen, A. H. Vuorimäki, and E. E. Ylinen, *J. Phys. C* **18**, 5033 (1985).

³⁸W. Häusler (to be published).

³⁹A. Hüller, *Z. Phys. B* **36**, 215 (1980).

⁴⁰T. H. Chao and D. F. Eggers, *J. Chem. Phys.* **66**, 970 (1977).

⁴¹Calculations of P. N. Gerlach along the Lines of Ref. 2 shows that CH_3Cl should undergo a phase transition to the same structure as CH_3I and CH_3Br around $T \approx 120$ K. This prediction will be checked.